Eur Arch Psychiatry Clin Neurosci (2011) 261:433–446
DOI 10.1007/s00406-010-0184-0

ORIGINAL PAPER

A visual [18F]FDG-PET rating scale for the differential diagnosis of frontotemporal lobar degeneration

Stefan Poljansky · Bernd Ibach · Barbara Hirschberger · Peter Männer · Hans Klünemann · Göran Hajak · Jörg Marienhagen

Received: 14 December 2009 / Accepted: 17 December 2010 / Published online: 5 January 2011

Abstract This study presents a visual rating scale for the assessment of cerebral [^{18}F]fluoro-2-deoxy-D-glucose positron emission tomography (FDG-PET) scans to characterize typical findings in dementias associated with frontotemporal lobar degeneration (FTLD) and to differentiate individual patients with FTLD compared to Alzheimer's disease (AD) and mild cognitive impairment (MCI). A total of 43 cerebral PET scans from patients with FTLD ($n = 16$, mean age 58.4 years), AD ($n = 16$, 59.9 years) and MCI ($n = 11$, 57.9 years) were analysed. Every PET data set was visually rated for seven brain regions on each hemisphere (frontal lobe, temporal lobe, parietal lobe, occipital lobe, basal ganglia, thalamus and cerebellum). The extent of the impairment in metabolism was classified as absent, mild, medium or strong. Using this four-stage visual rating scale, characteristic profiles of metabolic impairment in FTLD, AD, MCI and the FTLD-subgroup FTD ($n = 9$) could be demonstrated. Patients with FTLD showed a significantly lower metabolism in the left frontal lobe and in the left basal ganglia when compared to AD and to MCI. Complementary analyses using statistical parametric mapping (SPM2) supported the findings of the visual analysis. In detecting FTLD with visual rating, sensitivity/specificity was 81/94% compared to AD and 81/64% compared to MCI. Patients with FTD were correctly attributed to a diagnosis of FTLD with a sensitivity of 89%. This visual rating scale may facilitate the differential diagnosis of FTLD in clinical routine.

Keywords Positron emission tomography · Frontotemporal lobar degeneration · Semantic dementia · Progressive aphasia · Early-onset Alzheimer's disease · Presenile dementia

S. Poljansky (✉) · B. Ibach · H. Klünemann · G. Hajak
Department of Psychiatry, Psychosomatic Medicine and Psychotherapy, University of Regensburg, Universitätsstrasse 84, 93053 Regensburg, Germany
e-mail: stefan.poljansky@medbo.de

B. Hirschberger · P. Männer · J. Marienhagen
Department of Nuclear Medicine, University of Regensburg, 93053 Regensburg, Germany

Introduction

The group of dementias associated with frontotemporal lobar degeneration (FTLD) together with early-onset Alzheimer's disease (AD) represent the most prevalent early-onset dementia syndromes due to neurodegeneration. The FTLD group can be clinically characterized by two major features occurring early in the course of disease: gradual and progressive behavioural changes and gradual and progressive language dysfunction. According to these observations, three prototypic syndromes of FTLD have been defined [27] as frontotemporal dementia (FTD), semantic dementia (SemD) and progressive non-fluent aphasia (PA), although there is a considerable clinical and neuropathological overlap between these syndromes [2, 19]. FTLD may even present atypical symptoms [11], mimicking other psychiatric or neurologic disorders, including Alzheimer's disease.

Besides clinical assessment [34] and neuropsychological testing [47], differential diagnosis of FTLD may be supported by the use of cerebrospinal fluid analysis [1, 13, 21, 38], MRI-based structural brain imaging [20, 44] and functional brain imaging like single-photon emission computed tomography (SPECT) [4, 24, 44, 45] and

positron emission tomography (PET) [8, 12, 15, 17, 25, 28, 29, 37, 39, 40, 48].

[^{18}F]fluoro-2-deoxy-D-glucose-PET (FDG-PET) is an increasingly available technique for the diagnosis of patients with neurodegenerative cognitive disorders, which raises the issue of validating FDG-PET as a biomarker for FTLD. In a recent multicentre study, the rate of hospitalized patients with FTLD receiving a diagnostic cerebral PET scan was estimated at about 12% [11].

Burdette et al. [3] demonstrated that the accuracy of detecting AD with FDG-PET could be improved using a three-dimensional stereotactic surface projection technique (3-D SSP) instead of visual inspection of standard transaxial slices. Imabayashi et al. [14] found a higher ability of 3-D SSP compared to visual inspection to discriminate patients with early AD from healthy control subjects. For the differentiation of FTD and AD with FDG-PET, Foster et al. [6] reported a mean sensitivity of 73.2% and a mean specificity of 97.6% for FTD using visual interpretation of SSP images. In a further study, Van Laere et al. [43] evaluated the performance of different operator-independent SPECT analyses in diagnosing patients with cognitive impairment (12 AD, 2 multiinfarct dementias and 1 FTD). Using receiver operating characteristics (ROC), they showed the superiority of a voxel-wise region-growing technique [brain registration and analysis of SPECT studies (BRASS)] over visual analysis of SPECT scans, whereas SPM showed the lowest areas under the ROC curve. A comprehensive review of Patwardhan et al. [33] elucidated a high degree of heterogeneity in the specificity and sensitivity estimates in FDG-PET comparing AD to healthy controls as well as other causes of dementia. Previously, Newberg et al. [30] introduced a visual FDG-PET rating scale [Metabolic Imaging Severity Rating Scale (MISRS)] and showed a significant correlation between the MISRS and the Mini-Mental State Examination scores for AD ($n = 65$) and for frontal lobe dementia ($n = 16$), but MISRS failed to distinguish AD from frontal lobe dementia. In a recently published study, Mosconi et al. [25] examined 114 patients with mild cognitive impairment (MCI), 199 patients with AD and 98 patients with FTD using an automated voxel-based comparison of FDG-PET. By means of standardized disease-specific patterns of FDG uptake, they could correctly classify 95% of the AD patients and 94% of the FTLD patients, whereas patients with MCI showed a stronger heterogeneity in PET findings.

Against the background of the data available, the first aim of the present investigation was defined as a description of the hypometabolic brain regions that discriminate the FTLD group as one entity from AD or MCI. This objective will be traced by applying an easy-to-use new visual rating scale for the assessment of cerebral FDG-PET scans in daily clinical routine, providing an FTLD-specific metabolic profile. In a subgroup analysis, a specific metabolic profile will also be given for patients with the prototypic syndrome FTD. The second aim of the study was to differentiate individual patients with FTLD from patients with AD and MCI using this visual rating scale and to give data on sensitivity and specificity in the diagnosis of FTLD. Finally, statistical parametric mapping (SPM2) will be used to verify the results of the visual analysis.

Methods

Patients

We enrolled 51 patients with a clinical diagnosis of FTLD, AD or MCI in this study. All patients were recruited from the memory clinic of the Department of Psychiatry at the University of Regensburg, specialized in the diagnosis and treatment of rare forms of dementia.

Patients underwent a standard battery of examinations, including medical history, physical and neurological examination, screening laboratory tests, structural brain imaging (magnetic resonance imaging or cranial computed tomography) and a neuropsychological test battery, including Mini-Mental State Examination, Clock Drawing Test [41], activities of daily living (B-ADL, [10]) and frontal lobe tests, e.g. verbal fluency, frontal behavioural inventory (FBI) [18]. Most of the patients received an extended neuropsychological examination (e.g. CERAD battery [26], SIDAM [49]). A detailed logopedic assessment was available for a part of the patients with FTLD. Lumbar puncture was conducted in 30 patients (53% of the FTLD cases, 62% of the AD cases and 62% of the MCI cases), and cerebrospinal fluid tau, p-tau$_{181}$ and amyloid-beta$_{42}$ were measured [13]. For statistical analyses, SPSS 13.0 has been used. Exclusion criteria in all patients were a history of stroke or other major vascular lesions. No cases of severe dementia were included.

According to the below-mentioned criteria, 16 patients were classified as FTLD, 21 patients as AD and 11 patients as MCI by an experienced psychiatrist. Clinical diagnoses were reviewed by the team of our memory clinic, Department of Psychiatry at the University of Regensburg, including two psychiatrists, one neurologist and one nurse specialized in psychiatry.

FTLD diagnosis was made according to the criteria of Neary et al. [27]. Patients fulfilled the particular clinical core diagnostic features for at least one of the three prototypic syndromes of FTLD [frontotemporal dementia (FTD, $n = 9$), progressive non-fluent aphasia (PA, $n = 4$) and semantic dementia (SemD, $n = 3$)]. Two patients with FTD additionally showed a Parkinson's syndrome.

Probable AD ($n = 21$) was diagnosed according to the NINCDS-ADRDA criteria [23]. None of the AD patients fulfilled the internationally recommended criteria for the diagnosis of a probable dementia with Lewy bodies (DLB) [22].

For the diagnosis of MCI, various concepts have been proposed up to now [32, 35, 36, 46]. In this study, patients with MCI ($n = 11$) were classified according to the criteria of Winblad et al. [46]. Two patients were amnestic MCI, eight patients were multidomain MCI (amnestic), and one patient was single non-memory domain MCI.

Since brain atrophy is an age-dependent process, what may influence the results of functional brain imaging techniques, patients of comparable age were included. For the final analysis, in order to correct for the early age of onset in FTLD, we exclusively selected age-matched patients with early-onset AD ($n = 16$) from the pool of 21 patients with probable AD.

Image acquisition

After determination of the clinical diagnoses, all patients received a cerebral PET. Patients had fasted overnight for at least 9 h before PET scanning. To minimize interference due to movement, the patients' heads were fixed in a shell. Absorption correction was done by automated attenuation. PET studies were performed under resting conditions with eyes closed and ears unplugged. After a rest period of at least 15 min, about 150 MBq [18F]fluorodeoxyglucose was injected into an antecubital vein. Brain scanning was started about 30 min after the injection. Forty-seven slices of transversal positron emission tomographic images of the whole brain were collected (Siemens ECAT-EXACT). All patients were examined with the same PET scanner. Raw data sets were 256 × 256 × 47 pixel in size. Patients or their legal representatives had given their written consent prior to the PET scan. The analysis of the PET data was conducted in accordance with the guidelines of the local ethics committee.

Image analysis

Visual rating analysis

A hardcopy of every PET data set with all slices in the transversal plane was visually rated by an experienced physician for nuclear medicine (J. M.) and an psychiatrist (S. P.) for seven brain regions on each hemisphere (frontal lobe [including the anterior cingulate region], temporal lobe, parietal lobe [including the posterior cingulate region], occipital lobe, basal ganglia, thalamus and cerebellum) as defined anatomically, for nomenclature cf. Talairach and Tournoux [42]. The extent of the impairment in metabolism was classified as absent (0), mild (1), medium (2) or strong (3). For classification of the PET scans, an attempt of operationalization was made, and the respective criteria are shown in Table 1. The readers were blinded to the patients' names, clinical diagnoses and all results of structural brain imaging, physical examination, laboratory tests and neuropsychological testing. Three examples of classification are given in Fig. 1 (two patients with FTLD, one patient with AD). J. M. rated all PET scans without training. S. P. rated the PET scans after training: in a first pass, all PET scans were presented in random order. S. P. rated the respective scan and immediately could see the associated rating of J. M. This first pass was not used for the results section. Seven days after this training, S. P. again rated all scans presented in random order, blinded to the number of the scan and to the associated rating of J. M., followed by a re-rating further 7 days later.

For statistical analyses, SPSS 13.0 has been used. Median, minimum and maximum of visual rating in FTLD, FTD, AD and MCI were calculated. One-sided Mann–Whitney *U*-test was conducted to detect significant decreases in metabolism in FTLD, FTD and AD. For intrarater- and interrater-agreement analysis, Kendalls W was calculated; thereby, a value of $W = 1$ stands for best accordance between ratings.

Table 1 Criteria for classification of regional hypometabolism in PET

Level	PET findings
Brain regions: frontal lobe, temporal lobe, parietal lobe, occipital lobe, cerebellum	
0	No hypometabolism
1	Mild well-defined hypometabolism observable in more than one image
2	Prominent well-defined hypometabolism in more than one image *or* mild hypometabolism in up to 50% of the evaluated area
3	Prominent hypometabolism in at least 50% of the evaluated area
Brain regions: basal ganglia, thalamus	
0	No hypometabolism
1	Mild hypometabolism observable in more than one image
2	Hypometabolism in major parts of basal ganglia/thalamus
3	Basal ganglia/thalamus not clearly identifiable

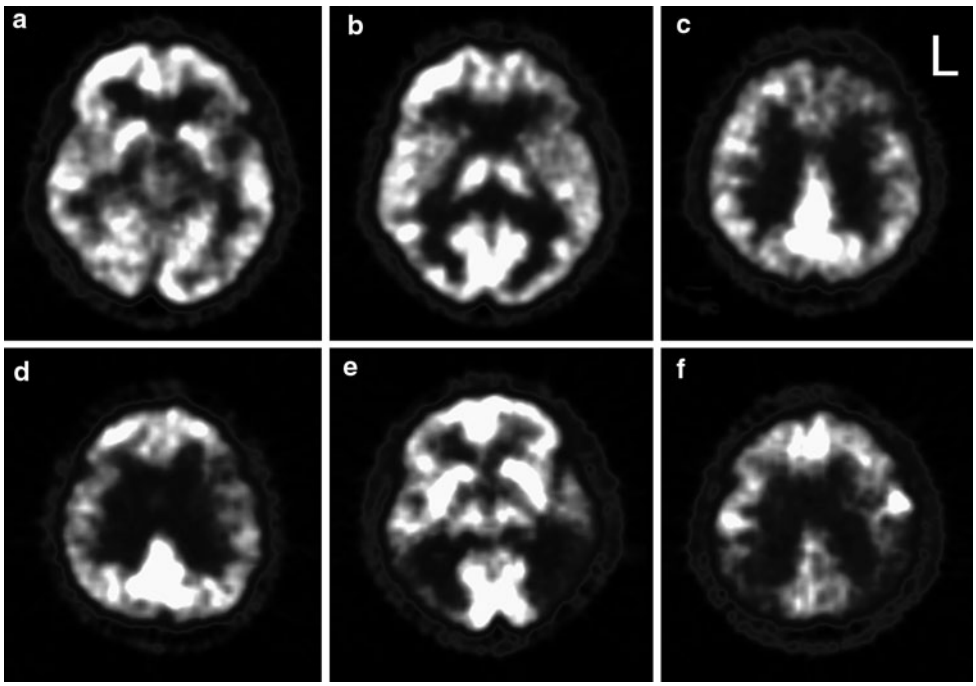

Fig. 1 **a–c** Fifty-one-year-old male patient with frontotemporal lobar degeneration (FTLD); hypometabolic regions: left basal ganglia (level 1, **a**), left thalamus (level 1, **b**), left frontal lobe (level 2, **a–c**) and left temporal lobe (level 2, **a–b**). **d** Sixty-three-year-old female patient with FTLD; isolated left frontal prominent well-defined hypometabolism (level 2). **e–f** Fifty-five-year-old female patient with Alzheimer's disease; hypometabolic regions (bilaterally): temporal lobes (level 3, **e**), occipital lobes (level 2, **e**) and parietal lobes (level 3, **f**)

Statistical parametric mapping

Additionally, statistical analysis was performed with statistical parametric mapping (SPM2) [7]. For the analysis with SPM2, image data were converted to the ANALYZE format, and all data sets of the 43 patients were used. Nine of the 16 AD PET scans and 7 of the 16 FTLD PET scans had been used for a previous analysis with SPM99 [37]. Data sets were normalized (voxel size $2.0 \times 2.0 \times 2.0$ mm) and smoothed (10 mm). Standard SPM2 configurations were used (PET models, compare populations [1 scan/subject, two-sample *t* test], proportional scaling to a global mean of 50, threshold masking to a global 0.8). Analysing FTLD versus MCI ($n = 16/11$), FTD versus MCI ($n = 9/11$) and AD versus MCI ($n = 16/11$), statistical tests were made at the $P < 0.0005$ level, uncorrected. In the analyses of FTLD versus AD ($n = 16/16$) and FTD versus AD ($n = 9/16$), *P* value was set to 0.05 and results were corrected for multiple comparisons (family-wise error, FWE). The extent threshold was set to 125 voxels. This threshold corresponds to a volume of 1.0 ml brain tissue and may be adequate to simulate a volume that can be detected in the visual inspection of a brain PET scan. *T*-contrasts were defined as "−1 1" to illustrate hypometabolism in patient group 1 versus group 2. As the resulting coordinates in SPM2 are given in the MNI (Montreal Neurological Institute) space, coordinates were transformed to the corresponding values of the standard brain of the Talairach Atlas [42] using a non-linear approach (http://www.mrc-cbu.cam.ac.uk/Imaging/Common/mnispace.shtml). Corresponding brain regions and Brodmann's areas were determined by using the talairach daemon client, version 2.0 (http://ric.uthscsa.edu/projects/talairachdaemon.html). Additionally, analogous analyses with SPM5 were conducted with identical general settings and identical thresholds for *P* values and cluster extent.

Results

Patients

Table 2 summarizes the clinical, neuropsychological and cerebrospinal fluid characteristics of the patients. The mean values for MMSE were significantly higher in the MCI group versus FTLD, the FTLD-subgroup FTD or AD. Those for the Clock drawing test were significantly lower in the MCI group versus FTLD, FTD or AD ($P < 0.05$, two-tailed Mann–Whitney *U*-test); in the Clock drawing test, a score of one stands for no impairment, and a score of six represents maximum impairment in visuoconstructive abilities. No significant differences were found for age ($P > 0.1$, unpaired *t* test) or gender ($P > 0.4$, two-tailed Fisher's exact test) between FTLD, FTD, AD and MCI.

Visual rating analysis

Median, minimum and maximum of visual rating in FTLD, the FTLD-subgroup FTD, AD and MCI are displayed in Table 3. Figure 2 shows the respective profiles of metabolic impairment in FTLD and in FTD compared to AD obtained by visual rating analysis. For the right

Table 2 Clinical characteristics of the subjects {mean (standard deviation)}

Diagnosis	FTLD	FTD	AD	MCI
Number of patients	16	9	16	11
Age (years)	58.4 (9.8)	55.3 (9.2)	59.9 (5.4)	57.9 (12.2)
Female/male	10/6	4/5	9/7	5/6
Clock drawing test	2.9 (1.6)	2.9 (1.5)	3.7 (1.3)	1.4 (0.7)
MMSE	22.8 (7.9)	23.6 (3.7)	20.8 (6.3)	27.9 (2.0)
Cerebrospinal fluid analysis				
Amyloid-beta$_{42}$ (pg/ml)	691 ($n = 9$)	756 ($n = 5$)	475 ($n = 11$)	793 ($n = 6$)
Tau (pg/ml)	376 ($n = 9$)	306 ($n = 5$)	648 ($n = 11$)	245 ($n = 6$)
Phospho-tau$_{181}$ (pg/ml)	56 ($n = 9$)	50 ($n = 5$)	94 ($n = 11$)	54 ($n = 5$)

MMSE Mini-Mental State Examination

Table 3 Median, minimum and maximum of visual rating of metabolism in FTLD, FTD, AD and MCI (Rating by J. M.)

Brain region	FTLD			FTD			AD			MCI		
	Med.	Min.	Max.	Med.	Min.	Max.	Med.	Min.	Max.	Med.	Min.	Max.
R. frontal lobe	0	0	3	0	0	3	0	0	2	0	0	2
R. temporal lobe	0	0	2	2	0	2	1	0	3	1	0	3
R. parietal lobe	0	0	2	0	0	2	2	0	3	1	0	2
R. occipital lobe	0	0	2	0	0	2	2	0	3	0	0	2
R. basal ganglia	0	0	2	0	0	2	0	0	2	0	0	0
R. thalamus	0	0	2	0	0	2	0	0	2	0	0	1
R. cerebellum	0	0	2	0	0	2	0	0	0	0	0	0
L. frontal lobe	2	0	3	2	0	3	0	0	2	0	0	3
L. temporal lobe	2	0	3	2	0	3	2	0	3	1	0	3
L. parietal lobe	2	0	3	0	0	3	2	0	3	1	0	2
L. occipital lobe	0	0	3	0	0	3	2	0	3	1	0	2
L. basal ganglia	1	0	2	1	0	2	0	0	2	0	0	1
L. thalamus	0	0	2	0	0	2	0	0	2	0	0	1
L. cerebellum	0	0	2	0	0	2	0	0	0	0	0	0

R right, *L* left, *Med* median, *Min* minimum, *Max* maximum

hemisphere, the median of metabolic impairment in FTLD is smaller than level 1 (mild impairment) for all brain regions, and no significant hypometabolism relative to AD can be detected (first column in the data field of Table 4). In our sample, AD is characterized by relatively symmetrical profiles of metabolic impairment between the right and left hemispheres, i.e. strong reduction in glucose metabolism temporo-parieto-occipitally (=level 2) and lack of hypometabolism in the frontal lobes, the basal ganglia, thalami and cerebellum. In contrast to these findings, there is a marked asymmetry of metabolic impairment between right and left hemispheres for FTLD in our sample. The left hemisphere shows a pronounced impairment (level 2) in the frontal, temporal and parietal lobes. A significant hypometabolism in FTLD compared to AD can be shown for the left frontal lobe and for the left basal ganglia (Fig. 2 and Table 4). The FTLD-subgroup FTD presents a significant left frontal hypometabolism, furthermore a bilateral temporal hypometabolism and a reduced metabolism for the left basal ganglia (Fig. 2 and Table 4).

Figure 3 demonstrates the profiles of metabolic impairment in FTLD and in FTD versus MCI obtained by visual rating analysis. The profile observed in MCI is approximately symmetrical as regards right and left hemispheres, with mild metabolic impairment in the temporal, parietal and occipital lobes and missing impairment in the frontal lobes, basal ganglia, thalami and cerebellum. These findings resemble the pattern observed in AD with an overall lower degree of impairment. A statistically significant hypometabolism in FTLD compared to MCI can be detected in the left frontal lobe and in the left basal ganglia. FTD presents a significant hypometabolism in the left frontal lobe when compared to MCI (Table 4).

Table 4 Brain regions of significantly decreased metabolism in FTLD and FTD when compared to AD or MCI, respectively, and in AD when compared to MCI obtained by visual analysis ($P < 0.05$, one-sided Mann–Whitney U-test)

	FTLD < AD	FTD < AD	FTLD < MCI	FTD < MCI	AD < MCI
Brain region					
R. frontal lobe	ns (ns)	ns (0.041)	ns (0.048)	ns (0.009)	ns (ns)
R. temporal lobe	– (–)	– (–)	– (ns)	ns (ns)	ns (ns)
R. parietal lobe	– (–)	– (–)	– (–)	– (–)	0.034 (0.044)
R. occipital lobe	– (–)	– (–)	– (–)	– (–)	0.035 (ns)
R. basal ganglia	ns (ns)	ns (ns)	ns (–)	ns (ns)	ns (–)
R. thalamus ns	(–)	ns (–)	ns (–)	ns (–)	– (–)
R. cerebellum	ns (ns)	ns (ns)	ns (ns)	ns (ns)	– (ns)
L. frontal lobe	<0.001 (0.005)	<0.001 (0.001)	0.001 (0.037)	0.003 (0.009)	– (–)
L. temporal lobe	– (–)	– (–)	ns (ns)	ns (ns)	ns (0.043)
L. parietal lobe	– (–)	– (–)	ns (–)	– (–)	0.037 (0.001)
L. occipital lobe	– (–)	– (–)	– (–)	– (–)	0.042 (ns)
L. basal ganglia	0.015 (ns)	ns (ns)	0.033 (ns)	ns (ns)	– (–)
L. thalamus	ns (ns)	ns (ns)	ns (ns)	ns (ns)	ns (ns)
L. cerebellum	ns (–)	ns (–)	ns (–)	ns (–)	– (–)

R right, *L* left, *ns* no significant decrease in metabolism, – no relative hypometabolism

Rating by J. M. (by S. P.)

As an internal control for the FTLD-related results, we performed a plausibility check by contrasting the AD versus the MCI group as outlined in Fig. 4 and Table 4, last column. The profiles of AD and MCI involve the same regions (temporal, parietal and occipital) in both groups with a stronger impairment in metabolism in AD when compared to the MCI group. Differences in metabolism were statistically significant for the right and left parietal and occipital lobes.

In a second step on a heuristic basis, decision criteria for classifying PET scans as FTLD or "non-FTLD" were developed (Fig. 5a). Using these criteria for the differentiation of FTLD and AD, sensitivity/specificity was 81/94% (Fig. 5b, rater: J. M.) and 63/94%, respectively (rater: S. P.). In the differentiation of FTLD and MCI, values for sensitivity/specificity were 81/64% (Fig. 5d, J. M.) and 63/73% (S. P.). The aforementioned decision criteria (Fig. 5a) were then applied to the FTLD-subgroup FTD (Fig. 5c, e), and patients with FTD were correctly attributed to a diagnosis of FTLD with a sensitivity of 89% (equivalent result J. M. and S. P.).

Data on interrater reliability and intrarater reliability are shown in Table 5. Interrater accordance was good (Kendalls $W > 0.75$) for the frontal lobes, temporal lobes, parietal lobes, occipital lobes, left thalamus, left basal ganglia and the right cerebellum, whereas accordance for the remaining three regions was lower. For intrarater analysis, accordance was better than those in interrater analysis (Kendalls $W > 0.80$; except for left cerebellum). Thus, all regions used for the decision criteria (left and right frontal lobes, left basal ganglia, right occipital lobe) showed a good reliability in the inter- and intrarater analysis.

Statistical parametric mapping

Complementary analyses using statistical parametric mapping (SPM2) were conducted to confirm the results of the visual analysis by objective measurement. In Tables 6, 7 and 8, coordinates of the local maxima are shown as given by the standard settings of SPM2. Figures 6, 7 and 8 display the corresponding regions in sagittal, coronal and transverse projections in the stereotaxic space of Talairach.

Table 6 and Fig. 6 characterize the regions A and B as significantly hypometabolic in FTLD and FTD, respectively, relative to AD obtained by use of SPM2. The marked hypometabolism in the left inferior frontal gyrus (A, B) extending to the middle frontal gyrus and to the left anterior insula (A) is consistent with the results of the visual analysis; the relative hypometabolism in the left basal ganglia shown in Fig. 2 could not be reproduced with the chosen parameters in SPM2.

Hypometabolic brain regions in FTLD and FTD, respectively, when compared to MCI are described in Table 7 and Fig. 7. Identification of regions C (left inferior frontal gyrus/left anterior insula) and D (left middle and inferior temporal gyrus) in FTLD is in full accordance with the results of the visual rating shown in Fig. 3. Likewise, hypometabolism left frontally in regions E, F and G reflects the results of the visual analysis in FTD. Parallel to the

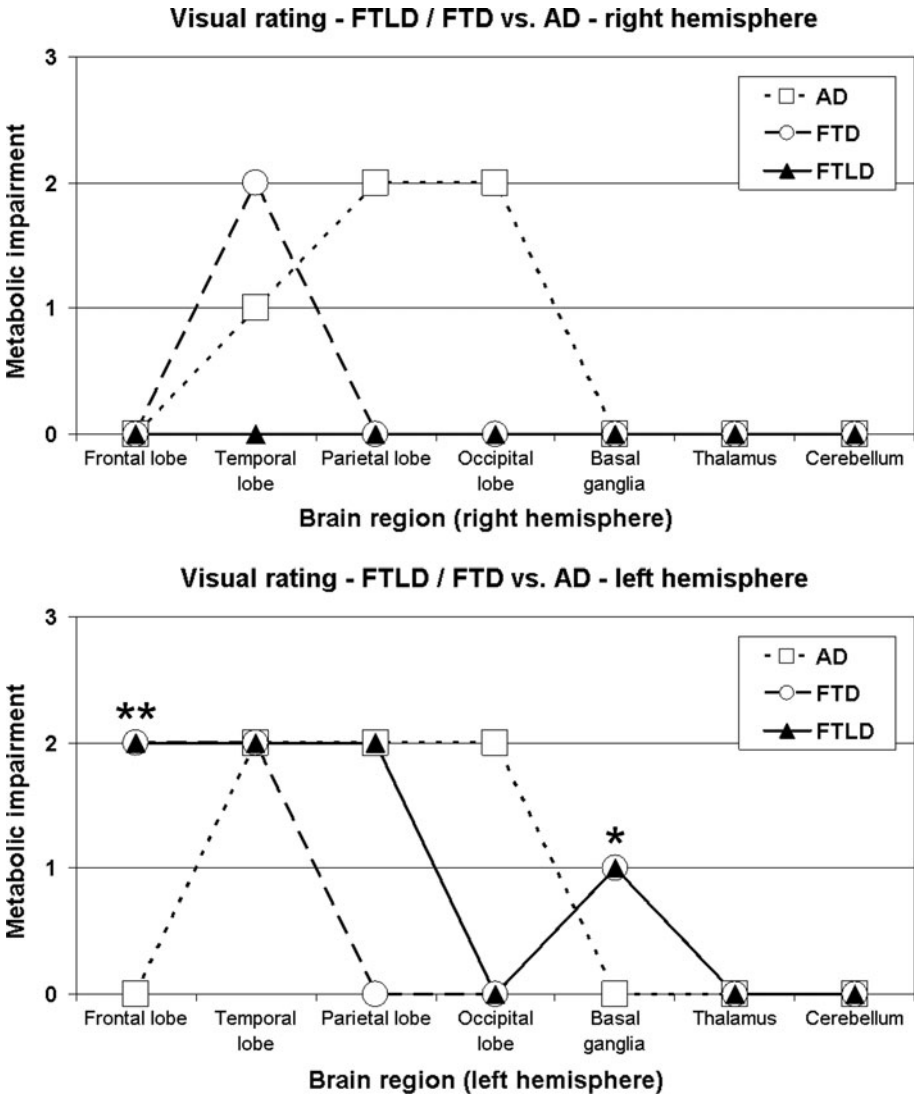

Fig. 2 Profiles of metabolic impairment in frontotemporal lobar degeneration (FTLD, $n = 16$), frontotemporal dementia (FTD, $n = 9$) and Alzheimer's disease (AD, $n = 16$). Impairment in metabolism was classified as absent (*0*), mild (*1*), medium (*2*) or strong (*3*) in all cases. The respective median is displayed. Note the asymmetry in impairment between right and left hemispheres in FTLD. (**$P < 0.005$, *$P < 0.05$, rating by J. M., see Table 4)

analyses versus AD, SPM2 again did not detect a significant hypometabolism in the left basal ganglia.

Table 8 and Fig. 8 finally specify regions of hypometabolism in AD compared to MCI obtained in the analysis with SPM2. In Fig. 8, regions H, I and J with typically reduced glucose utilization in early AD are highlighted. The left Brodmann area (BA) 21 represents a region affected in AD as well as in FTLD (Tables 7, 8). Further on, in concordance with the visual rating, a reduced metabolism in the right occipital lobe in AD could be proved by use of SPM2 (BA 19, region J). The left hemispheric region H is also located in close vicinity of the occipital lobe (BA 19), which again supports the finding in the visual rating scale. SPM2, as well as visual analysis, showed the profile of hypometabolism in AD to be symmetric in both hemispheres.

The results obtained with the analogous analyses using SPM5 revealed identical regions of hypometabolism and identical cluster sizes when compared to the analyses with SPM2.

Discussion

With the data set presented here, we are introducing a visual rating scale for FDG-PET scans that may facilitate the differential diagnosis of dementias associated with frontotemporal lobar degeneration (FTLD). Below, we would like to stress two particular features of our explorative study. First, we made a direct comparison of FTLD with subjects diagnosed as having mild cognitive impairment (MCI) or Alzheimer's disease (AD). Using these data, we proposed decision criteria for the diagnosis of FTLD based on visual rating. Second, we conducted a comparative application of subjective visual rating versus group-related objective SPM-based analysis. Our major findings

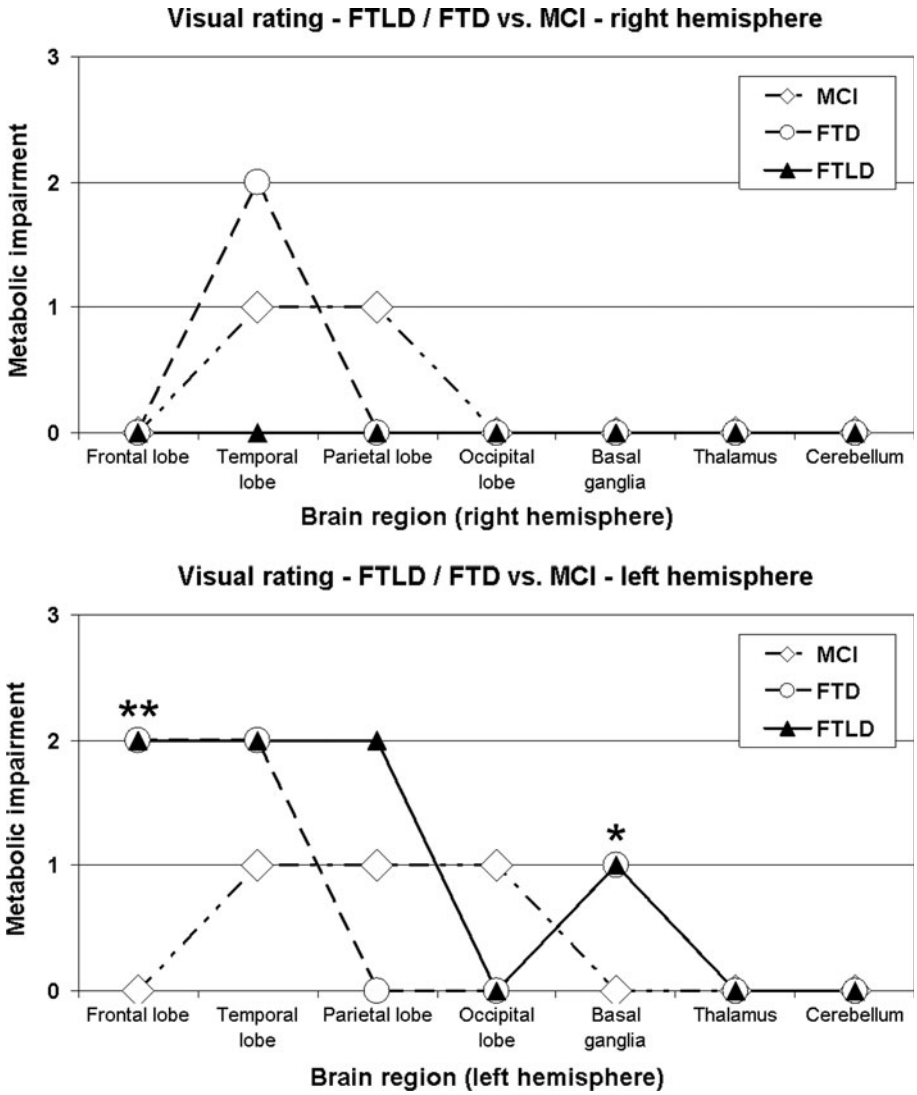

Fig. 3 Profiles of metabolic impairment in FTLD ($n = 16$), FTD ($n = 9$) and mild cognitive impairment (MCI, $n = 11$). Impairment in metabolism was classified as absent (*0*), mild (*1*), medium (*2*) or strong (*3*) in all cases. The respective median is displayed. (**$P < 0.005$, *$P < 0.05$, rating by J. M., see Table 4)

are a close homogeneity between the results of both methodological approaches and the high capacity of visual analysis to discriminate the diagnostic entities under investigation.

In comparison with AD, MMSE is affected later during disease course for most of the patients with FTLD, but due to language dysfunction and impairment in verbal communication, scores in MMSE may be lowered in patients with FTLD even at the beginning of the disease. In our study, patients with AD scored worse in MMSE compared to FTLD or compared to the FTLD-subgroup FTD, even if the differences in MMSE did not reach significance. The elevated standard deviation of MMSE in the FTLD group reflects the spectrum of severity of disease. Compared to patients with FTLD, patients with AD have lowered visuoconstructive abilities early in the course of disease. Consistent with this, the AD patients in our study revealed stronger impairment in the Clock drawing test compared to the patients with FTLD or compared to the patients with FTD. In summary, we argue that patients with FTLD or FTD and patients with AD suffer from comparable severity of dementia in our study.

Typical FDG-PET findings in FTLD are considered distinct frontal or frontotemporal metabolic impairment [9] and emphasize the left insula, the left inferior frontal gyrus and bilaterally the medial frontal gyrus as contrasting core regions compared to AD [12, 37]. Adjacent metabolic decline for the parietal and the medial temporal regions as well as subcortical structures (thalamus, basal ganglia) has been described (cf. review by Ishii [16]). Similar to a previous region-of-interest analysis [15], we found a significant decrease in glucose metabolism in the left inferior frontal gyrus and in the left basal ganglia in our FTLD sample. An involvement of the basal ganglia in frontotemporal dementia (FTD) has also been reported early (stage 2) in the course of the disease in a neuropathological

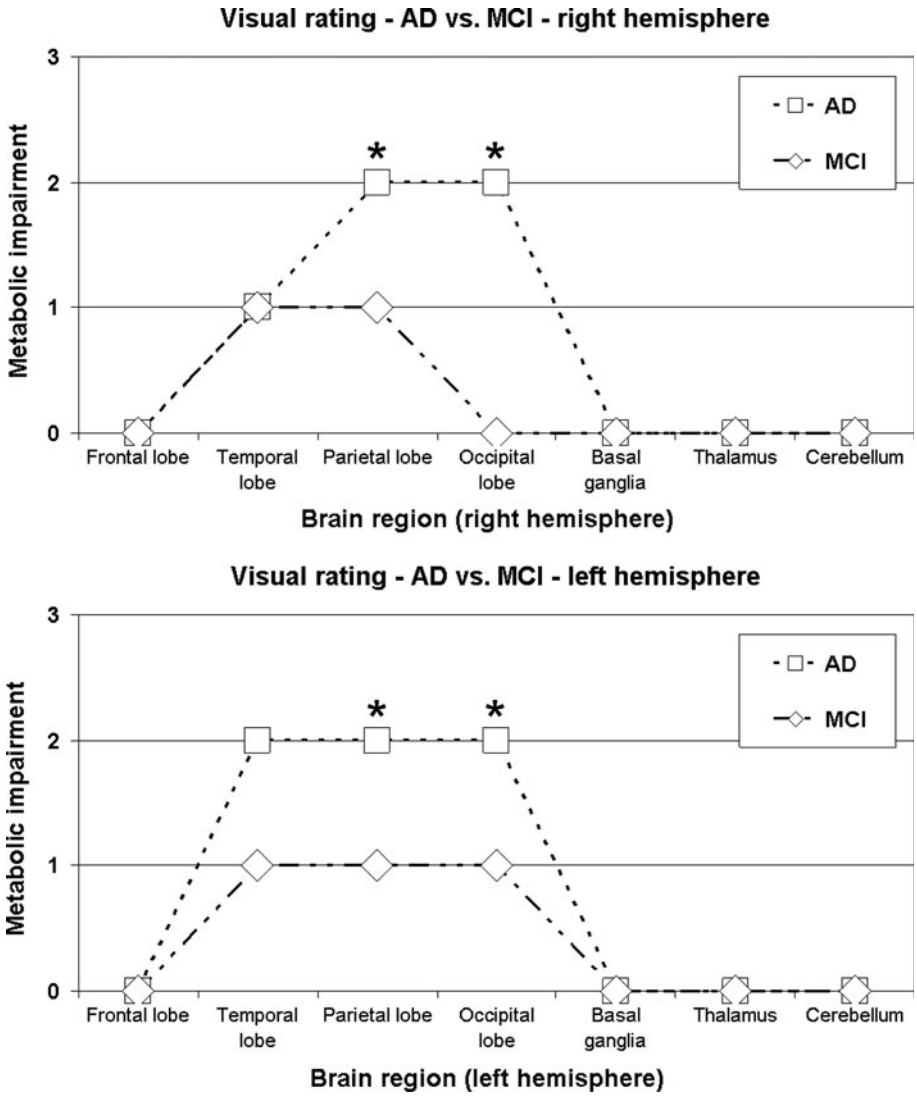

Fig. 4 Profiles of metabolic impairment in AD ($n = 16$) and MCI ($n = 11$). Impairment in metabolism was classified as absent (0), mild (1), medium (2) or strong (3) in all cases. The respective median is displayed. Note the comparatively strong symmetry in impairment between right and left hemispheres in AD and MCI as well as the overall lower degree of impairment in MCI. (*$P < 0.05$, rating by J. M., see Table 4)

study [2]. Our findings failed to show an affection of the thalami in FTLD, which is contrary to the results of Ishii et al. [15], who detected a significant metabolic impairment in this region. This may be explained by several potentially confounding circumstances. Involvement of the deep brain nuclei may depend on disease stages, sample size and clinical variants of the disease. In our FTLD sample, only three patients showed a mild sinistral thalamic hypometabolism and two patients showed a moderate one. Furthermore, we occasionally observed FTLD cases in our clinic with severe analgesia and concomitant reduced thalamic glucose metabolism. Random inclusion of such patients into studies may influence results, particularly when derived from relatively small sample sizes. In a further multicentre SPM99-based FDG-PET study, 29 patients with FTD were compared to 11 healthy controls [17], showing amongst others a significant hypometabolism in the left inferior parietal lobule, the bilateral insula and the left putamen and globus pallidus, moreover stating that frontal hypometabolism was more prominent in the left hemisphere than in the right, which again is consistent with our results.

A SPM-based FDG-PET study that contrasted glucose metabolism in progressive non-fluent aphasia (PA) relative to AD revealed a single impaired region centred over the left anterior insula [28]. Comparing PA to control subjects showed additional metabolic impairment for the frontal opercular region. These results are fully concordant with our SPM-based observations in the FTLD group comprising four cases with PA. In a further study, a marked metabolic impairment for the left lateral temporal lobe (BA 20 and BA 21) in patients with PA has been identified [48], which again matches our results with SPM2, further supporting the visual assessment results. Ancillary identification of a distinct left parietal hypometabolism in PA might match with our own observation of a left parietal non-

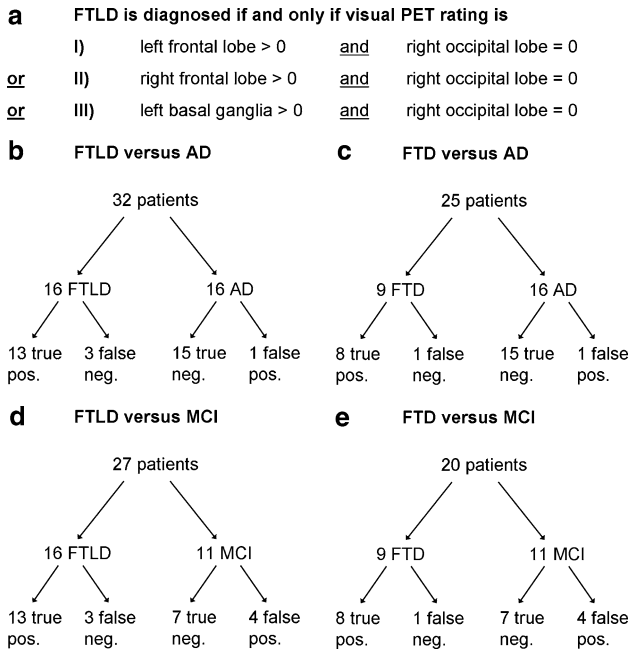

Fig. 5 **a** Decision criteria for the diagnosis of FTLD based on the results of visual PET rating. **b** Application of these criteria for discrimination between FTLD and AD, **c** between FTD and AD, **d** between FTLD and MCI, **e** between FTD and MCI. *Pos* positives, *neg* negatives

Table 5 Interrater analysis and intrarater analysis of visual rating. Kendalls *W* is shown for each region (*$P < 0.05$)

Brain region	Interrater analysis	Intrarater analysis
R. frontal lobe	0.816*	0.929*
R. temporal lobe	0.845*	0.905*
R. parietal lobe	0.871*	0.894*
R. occipital lobe	0.754*	0.884*
R. basal ganglia	0.587	0.931*
R. thalamus	0.598	0.890*
R. cerebellum	0.824*	0.825*
L. frontal lobe	0.865*	0.892*
L. temporal lobe	0.887*	0.945*
L. parietal lobe	0.854*	0.959*
L. occipital lobe	0.811*	0.943*
L. basal ganglia	0.768*	0.886*
L. thalamus	0.753*	0.949*
L. cerebellum	0.5	–

R right, *L* left, – no calculation, in both ratings S. P. in all cases rated "0" (no hypometabolism) for the left cerebellum

significant hypometabolism in the visual rating of the FTLD group. These findings may provide insight into the regional pattern of cortical metabolic impairment in PA, but may be compensated in the differential diagnosis to AD, where the parietal lobe is also strongly affected. This issue is supplemented by clinical evidence for the existence of in-between syndromes as regards PA and AD that simultaneously express predominant aphasia and further cognitive impairment.

In addition, the observed left temporal hypometabolism in FTLD in the visual rating scale presented here certainly will be influenced by those patients that have been diagnosed as having semantic dementia (SemD). This perception is supported by a recent FDG-PET study describing regions of hypometabolism in SemD for bilateral temporal lobes, more extensive on the left side and maximum in the poles and ventro-rostral surface [29].

Mild to moderate stages of AD are characterized by a reduction in metabolism in the parietotemporal region, the posterior cingulate and precuneus in contrast to a relatively preserved metabolism in the sensorimotor cortices, primary visual cortices, basal ganglia, thalamus and cerebellum [9, 16]. Our results using visual analysis and SPM2 are in full accordance with this known pattern of impairment. However, it may be surprising to see such a pronounced hypometabolism in the visual rating of the occipital lobes in AD and—to a lower degree—even in MCI. We explain this finding in AD by a hypometabolic region extending from the parietal lobe to the most anterior parts of the occipital lobe (BA 19), according to our results with SPM2. In a complementary study by Foster et al. [5], a metabolic involvement of the anterior occipital lobes in AD was reported, and impaired occipital metabolism in AD was detailed in further investigations (secondary visual cortex [31], right BA 19 [48], right BA 18 [29]). Another explanation may be an overlap with Lewy body pathology. However, none of our patients with AD fulfilled the criteria for the diagnosis of a probable DLB.

Eight of the eleven patients with MCI were cognitively impaired in multiple domains (including episodic working memory impairment in all cases). Thus, this group may be considered at risk for incipient AD, which might explain the congruency to the visual rating profiles of AD. We are aware of potentially interspersed patients with FTLD that may also experience MCI during the early stage of the disease. If the lower prevalence [11] and a possibly distinct MCI profile from early AD are considered to be anticipated, there will be a reduced probability for the unintentional inclusion of patients with FTLD.

A major limitation of our results is the exploratory character of this study. We are aware that the visual rating system was derived from the data set provided. It would therefore be desirable and a valuable approach to verify these preliminary results by a prospective controlled study design. Application of fine tuning for the affected frontal and temporal regions beyond the lobar anatomy appears to be inappropriate. This would probably lead to a pseudo-accuracy that could not really be achieved in a single case analysis. Due to the low numbers of patients in the PA and

Table 6 Brain regions with significant hypometabolism in patients with FTLD ($n = 16$) and in patients with FTD ($n = 9$) compared to AD ($n = 16$), analysis with SPM2

Brain region	BA	MNI-coordinates			Cluster size
		x	*y*	*z*	
FTLD					
A					
L. inferior and middle frontal gyrus	47	−42	30	0	227
L. inferior and middle frontal gyrus, l. anterior insula	47, 45	−34	30	2	
FTD					
B					
L. inferior frontal gyrus	47	−44	28	0	170

Results were thresholded at an FWE-corrected $P < 0.05$ (for voxel height). Extent threshold was set to a cluster size of 125 voxels, corresponding to 1.0 ml brain tissue. MNI-coordinates of local maxima (*x y z*) are stated in mm. *L* left, *BA* Brodmann area

Table 7 Brain regions with significant hypometabolism in patients with FTLD ($n = 16$) and in patients with FTD ($n = 9$) compared to MCI ($n = 11$), analysis with SPM2

Brain region	BA	MNI-coordinates			Cluster size
		x	*y*	*z*	
FTLD					
C					
L. anterior insula, l. inferior frontal gyrus	13, 45, 47	−36	20	6	190
D					
L. middle temporal gyrus	21	−66	−32	−14	155
L. inferior temporal gyrus	20	−64	−24	−26	
FTD					
E					
L. middle frontal gyrus	6	−28	6	70	664
L. middle frontal gyrus	8	−28	16	48	
L. superior frontal gyrus	6	−18	24	58	
F					
L. inferior frontal gyrus	45, 9	−56	20	24	222
L. middle frontal gyrus	9	−50	22	36	
L. middle frontal gyrus	46	−52	28	26	
G					
L. inferior frontal gyrus	47	−42	26	−14	315
L. inferior frontal gyrus, l. anterior insula	13, 45	−38	22	6	

Results were thresholded at an uncorrected $P < 0.0005$ (for voxel height). Extent threshold was set to a cluster size of 125 voxels, corresponding to 1.0 ml brain tissue. MNI-coordinates of local maxima (*x y z*) are stated in mm. *L* left, *BA* Brodmann area

in the SemD group, we could not picture the differences in glucose metabolism between these prototypic FTLD syndromes each and AD or MCI. As there is a clinical overlap in-between the prototypic FTLD syndromes and as these diseases may underlie a common pathology, we nevertheless regard the examination of our naturalistic FTLD group as a useful trace. Moreover, our analysis of the FTLD-subgroup FTD shows a clear consistency of the results. The analyses with the "pure" FTD group confirmed the main statements obtained for the whole FTLD group. This is first the correspondence of the relevant hypometabolic regions left frontal and left basal ganglia similar in FTLD and in FTD. Second, our analyses showed that the decision criteria for the diagnosis of FTLD based on visual PET rating are valid in particular for the subgroup of patients with "pure" FTD.

Summarizing our results, we have introduced a new and easy-to-use visual rating scale for FDG-PET scans here, which may enable clinicians to identify a characteristic asymmetric metabolic profile in patients with suspected FTLD. This pattern is distinct from those of early-onset AD and MCI. On a heuristic basis, we proposed decision criteria

Table 8 Brain regions with significant hypometabolism in patients with AD ($n = 16$) compared to MCI ($n = 11$), analysis with SPM2

Brain region	BA	MNI-coordinates			Cluster size
		x	*y*	*z*	
AD					
H					
L. angular gyrus, l. superior and middle temporal gyrus, l. supramarginal gyrus, l. precuneus	39	−42	−62	30	2,329
L. middle and inferior temporal gyrus	37, 21	−58	−46	−8	
L. middle temporal gyrus	21	−58	−32	−14	
I					
L. and r. cingulate gyrus, l. and r. precuneus, l. and r. posterior cingulate	31, 23, 7	−2	−54	28	1,866
R. and l. cingulate gyrus	31, 23	2	−32	36	
J					
R. superior and middle temporal gyrus, r. occipital lobe, r. supramarginal gyrus	39, 22, 19, 40	54	−60	18	1,421

Results were thresholded at an uncorrected $P < 0.0005$ (for voxel height). Extent threshold was set to a cluster size of 125 voxels, corresponding to 1.0 ml brain tissue. MNI-coordinates of local maxima (*x y z*) are stated in mm. *R* right, *L* left, *BA* Brodmann area

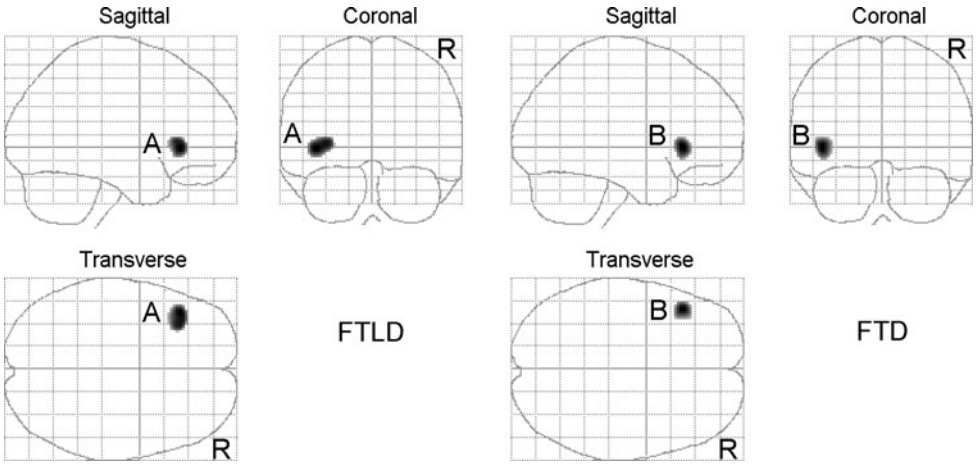

Fig. 6 Brain regions with significant hypometabolism in the patients with FTLD ($n = 16$) compared to the patients with AD ($n = 16$) and in the patients with FTD ($n = 9$) compared to AD

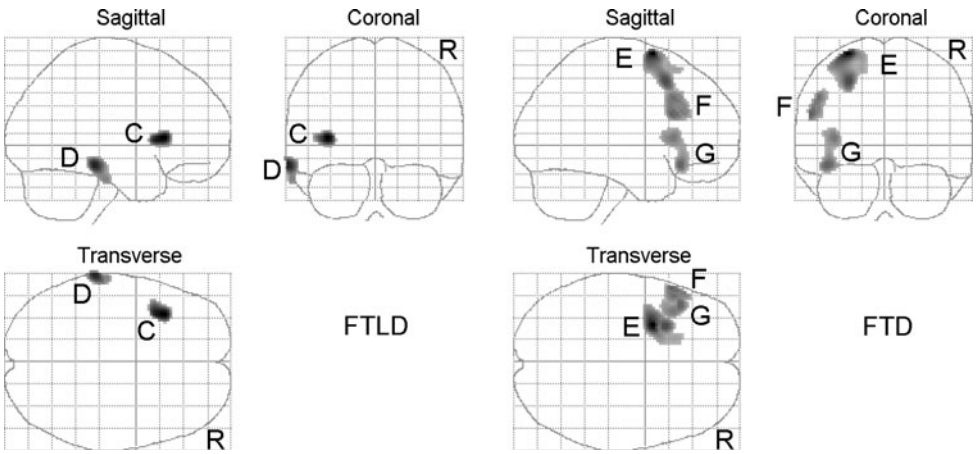

Fig. 7 Brain regions with significant hypometabolism in the patients with FTLD ($n = 16$) compared to the patients with MCI ($n = 11$) and in the patients with FTD ($n = 9$) compared to MCI

for the diagnosis of FTLD based on visual rating. Applying these criteria, individual patients could be classified as FTLD or "non-FTLD" with sensitivity/specificity values of [63–81%]/94% compared to AD and values of [63–81%]/[64–73%] compared to MCI. Applying the decision criteria to the FTLD-subgroup FTD, patients with FTD were

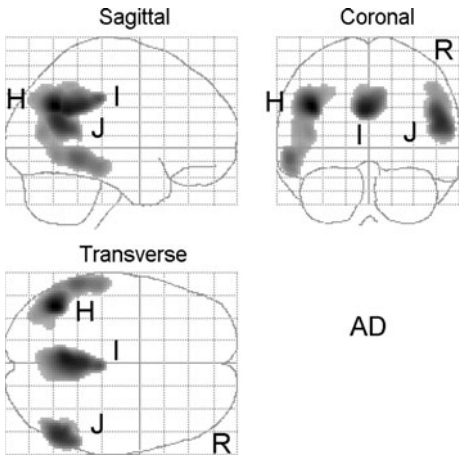

Fig. 8 Brain regions with significant hypometabolism in the patients with AD ($n = 16$) compared to the patients with MCI ($n = 11$)

correctly attributed to a diagnosis of FTLD with a sensitivity of 89%. Hypometabolism accentuated in the left frontal lobe and possibly the left basal ganglia may be most suitable to support the diagnosis of FTLD in clinical routine, whereas the role of the thalamus requires clarification.

References

1. Bibl M, Mollenhauer B, Wolf S, Esselmann H, Lewczuk P, Kornhuber J, Wiltfang J (2007) Reduced CSF carboxyterminally truncated Abeta peptides in frontotemporal lobe degenerations. J Neural Transm 114:621–628
2. Broe M, Hodges JR, Schofield E, Shepherd CE, Kril JJ, Halliday GM (2003) Staging disease severity in pathologically confirmed cases of frontotemporal dementia. Neurology 60: 1005–1011
3. Burdette JH, Minoshima S, Vander Borght T, Tran DD, Kuhl DE (1996) Alzheimer disease: improved visual interpretation of PET images by using three-dimensional stereotaxic surface projections. Radiology 198:837–843
4. Charpentier P, Lavenu I, Defebvre L, Duhamel A, Lecouffe P, Pasquier F, Steinling M (2000) Alzheimer's disease and frontotemporal dementia are differentiated by discriminant analysis applied to (99m)Tc HmPAO SPECT data. J Neurol Neurosurg Psychiatry 69:661–663
5. Foster NL, Chase TN, Mansi L, Brooks R, Fedio P, Patronas NJ, Di Chiro G (1984) Cortical abnormalities in Alzheimer's disease. Ann Neurol 16:649–654
6. Foster NL, Heidebrink JL, Clark CM, Jagust WJ, Arnold SE, Barbas NR, DeCarli CS, Turner RS, Koeppe RA, Higdon R, Minoshima S (2007) FDG-PET improves accuracy in distinguishing frontotemporal dementia and Alzheimer's disease. Brain 130:2616–2635
7. Friston KJ, Frith CD, Liddle PF, Frackowiak RS (1991) Comparing functional (PET) images: the assessment of significant change. J Cereb Blood Flow Metab 11:690–699
8. Garraux G, Salmon E, Degueldre C, Lemaire C, Laureys S, Franck G (1999) Comparison of impaired subcortico-frontal metabolic networks in normal aging, subcortico-frontal dementia, and cortical frontal dementia. Neuroimage 10:149–162
9. Herholz K (2003) PET studies in dementia. Ann Nucl Med 17:79–89
10. Hindmarch I, Lehfeld H, de Jongh P, Erzigkeit H (1998) The bayer activities of daily living scale (B-ADL). Dement Geriatr Cogn Disord 9(Suppl 2):20–26
11. Ibach B, Koch H, Koller M, Wolfersdorf M, Workgroup for Geriatric Psychiatry of the Psychiatric State Hospitals of Germany, Workgroup for Clinical Research of the Psychiatric State Hospitals of Germany (2003) Hospital admission circumstances and prevalence of frontotemporal lobar degeneration: a multicenter psychiatric state hospital study in Germany. Dement Geriatr Cogn Disord 16:253–264
12. Ibach B, Poljansky S, Marienhagen J, Sommer M, Männer P, Hajak G (2004) Contrasting metabolic impairment in frontotemporal degeneration and early onset Alzheimer's disease. Neuroimage 23:739–743
13. Ibach B, Binder H, Dragon M, Poljansky S, Haen E, Schmitz E, Koch H, Putzhammer A, Kluenemann H, Wieland W, Hajak G (2006) Cerebrospinal fluid tau and beta-amyloid in Alzheimer patients, disease controls and an age-matched random sample. Neurobiol Aging 27:1202–1211
14. Imabayashi E, Matsuda H, Asada T, Ohnishi T, Sakamoto S, Nakano S, Inoue T (2004) Superiority of 3-dimensional stereotactic surface projection analysis over visual inspection in discrimination of patients with very early Alzheimer's disease from controls using brain perfusion SPECT. J Nucl Med 45:1450–1457
15. Ishii K, Sakamoto S, Sasaki M, Kitagaki H, Yamaji S, Hashimoto M, Imamura T, Shimomura T, Hirono N, Mori E (1998) Cerebral glucose metabolism in patients with frontotemporal dementia. J Nucl Med 39:1875–1878
16. Ishii K (2002) Clinical application of positron emission tomography for diagnosis of dementia. Ann Nucl Med 16:515–525
17. Jeong Y, Cho SS, Park JM, Kang SJ, Lee JS, Kang E, Na DL, Kim SE (2005) 18F-FDG PET findings in frontotemporal dementia: an SPM analysis of 29 patients. J Nucl Med 46:233–239
18. Kertesz A, Davidson W, Fox H (1997) Frontal behavioral inventory: diagnostic criteria for frontal lobe dementia. Can J Neurol Sci 24:29–36
19. Kertesz A, McMonagle P, Blair M, Davidson W, Munoz DG (2005) The evolution and pathology of frontotemporal dementia. Brain 128:1996–2005
20. Kitagaki H, Mori E, Yamaji S, Ishii K, Hirono N, Kobashi S, Hata Y (1998) Frontotemporal dementia and Alzheimer disease: evaluation of cortical atrophy with automated hemispheric surface display generated with MR images. Radiology 208:431–439
21. Lewczuk P, Hornegger J, Zimmermann R, Otto M, Wiltfang J, Kornhuber J (2008) Neurochemical dementia diagnostics: assays in CSF and blood. Eur Arch Psychiatry Clin Neurosci 258(Suppl 5):44–49
22. McKeith IG, Galasko D, Kosaka K, Perry EK, Dickson DW, Hansen LA, Salmon DP, Lowe J, Mirra SS, Byrne EJ, Lennox G, Quinn NP, Edwardson JA, Ince PG, Bergeron C, Burns A, Miller BL, Lovestone S, Collerton D, Jansen EN, Ballard C, de Vos RA, Wilcock GK, Jellinger KA, Perry RH (1996) Consensus guidelines for the clinical and pathologic diagnosis of dementia with Lewy bodies (DLB): report of the consortium on DLB international workshop. Neurology 47:1113–1124
23. McKhann G, Drachman D, Folstein M, Katzman R, Price D, Stadlan EM (1984) Clinical diagnosis of Alzheimer's disease: report of the NINCDS-ADRDA Work Group under the auspices of department of health and human services task force on Alzheimer's disease. Neurology 34:939–944
24. Miller BL, Ikonte C, Ponton M, Levy M, Boone K, Darby A, Berman N, Mena I, Cummings JL (1997) A study of the Lund-Manchester research criteria for frontotemporal dementia:

clinical and single-photon emission CT correlations. Neurology 48:937–942
25. Mosconi L, Tsui WH, Herholz K, Pupi A, Drzezga A, Lucignani G, Reiman EM, Holthoff V, Kalbe E, Sorbi S, Diehl-Schmid J, Perneczky R, Clerici F, Caselli R, Beuthien-Baumann B, Kurz A, Minoshima S, de Leon MJ (2008) Multicenter standardized 18F-FDG PET diagnosis of mild cognitive impairment, Alzheimer's disease, and other dementias. J Nucl Med 49:390–398
26. Morris JC, Heyman A, Mohs RC, Hughes JP, van Belle G, Fillenbaum G, Mellits ED, Clark C (1989) The consortium to establish a registry for Alzheimer's disease (CERAD). Part I. clinical and neuropsychological assessment of Alzheimer's disease. Neurology 39:1159–1165
27. Neary D, Snowden JS, Gustafson L, Passant U, Stuss D, Black S, Freedman M, Kertesz A, Robert PH, Albert M, Boone K, Miller BL, Cummings J, Benson DF (1998) Frontotemporal lobar degeneration: a consensus on clinical diagnostic criteria. Neurology 51:1546–1554
28. Nestor PJ, Graham NL, Fryer TD, Williams GB, Patterson K, Hodges JR (2003) Progressive non-fluent aphasia is associated with hypometabolism centred on the left anterior insula. Brain 126:2406–2418
29. Nestor PJ, Fryer TD, Hodges JR (2006) Declarative memory impairments in Alzheimer's disease and semantic dementia. Neuroimage 30:1010–1020
30. Newberg A, Cotter A, Udeshi M, Alavi A, Clark C (2003) A metabolic imaging severity rating scale for the assessment of cognitive impairment. Clin Nucl Med 28:565–570
31. Newberg A, Cotter A, Udeshi M, Brinkman F, Glosser G, Alavi A, Clark C (2003) Brain metabolism in the cerebellum and visual cortex correlates with neuropsychological testing in patients with Alzheimer's disease. Nucl Med Commun 24:785–790
32. Palmer K, Fratiglioni L, Winblad B (2003) What is mild cognitive impairment? Variations in definitions and evolution of nondemented persons with cognitive impairment. Acta Neurol Scand Suppl 179:14–20
33. Patwardhan MB, McCrory DC, Matchar DB, Samsa GP, Rutschmann OT (2004) Alzheimer disease: operating characteristics of PET—a meta-analysis. Radiology 231:73–80
34. Perneczky R, Pohl C, Bornschein S, Förstl H, Kurz A, Diehl-Schmid J (2009) Accelerated clinical decline in well-educated patients with frontotemporal lobar degenerations. Eur Arch Psychiatry Clin Neurosci 259:362–367
35. Petersen RC, Doody R, Kurz A, Mohs RC, Morris JC, Rabins PV, Ritchie K, Rossor M, Thal L, Winblad B (2001) Current concepts in mild cognitive impairment. Arch Neurol 58:1985–1992
36. Petersen RC, Morris JC (2005) Mild cognitive impairment as a clinical entity and treatment target. Arch Neurol 62:1160–1163
37. Poljansky S, Ibach B, Vogel M, Männer P, Marienhagen J, Hajak G (2004) Unterschiede im zerebralen Glukosestoffwechsel zwischen frontotemporaler lobärer Degeneration und der Alzheimer-Krankheit. Psychiatr Prax 31(Suppl 1):73–75
38. Riemenschneider M, Wagenpfeil S, Diehl J, Lautenschlager N, Theml T, Heldmann B, Drzezga A, Jahn T, Förstl H, Kurz A (2002) Tau and Abeta42 protein in CSF of patients with frontotemporal degeneration. Neurology 58:1622–1628
39. Salmon E, Garraux G, Delbeuck X, Collette F, Kalbe E, Zuendorf G, Perani D, Fazio F, Herholz K (2003) Predominant ventromedial frontopolar metabolic impairment in frontotemporal dementia. Neuroimage 20:435–440
40. Salmon E, Kerrouche N, Herholz K, Perani D, Holthoff V, Beuthien-Baumann B, Degueldre C, Lemaire C, Luxen A, Baron JC, Collette F, Garraux G (2005) Decomposition of metabolic brain clusters in the frontal variant of frontotemporal dementia. Neuroimage 30:871–878
41. Shulman KI (2000) Clock-drawing: is it the ideal cognitive screening test? Int J Geriatr Psychiatry 15:548–561
42. Talairach J, Tournoux P (1988) Coplanar stereotaxic atlas of the human brain. 3-dimensional proportional system: an approach to cerebral imaging. Thieme, Stuttgart
43. Van Laere KJ, Warwick J, Versijpt J, Goethals I, Audenaert K, Van Heerden B, Dierckx R (2002) Analysis of clinical brain SPECT data based on anatomic standardization and reference to normal data: an ROC-based comparison of visual, semiquantitative, and voxel-based methods. J Nucl Med 43:458–469
44. Varma AR, Adams W, Lloyd JJ, Carson KJ, Snowden JS, Testa HJ, Jackson A, Neary D (2002) Diagnostic patterns of regional atrophy on MRI and regional cerebral blood flow change on SPECT in young onset patients with Alzheimer's disease, frontotemporal dementia and vascular dementia. Acta Neurol Scand 105:261–269
45. Varrone A, Pappata S, Caraco C, Soricelli A, Milan G, Quarantelli M, Alfano B, Postiglione A, Salvatore M (2002) Voxel-based comparison of rCBF SPET images in frontotemporal dementia and Alzheimer's disease highlights the involvement of different cortical networks. Eur J Nucl Med Mol Imag 29:1447–1454
46. Winblad B, Palmer K, Kivipelto M, Jelic V, Fratiglioni L, Wahlund LO, Nordberg A, Backman L, Albert M, Almkvist O, Arai H, Basun H, Blennow K, de Leon M, DeCarli C, Erkinjuntti T, Giacobini E, Graff C, Hardy J, Jack C, Jorm A, Ritchie K, van Duijn C, Visser P, Petersen RC (2004) Mild cognitive impairment–beyond controversies, towards a consensus: report of the international working group on mild cognitive impairment. J Intern Med 256:240–246
47. Yamada M, Ueda K, Namiki C, Hirao K, Hayashi T, Ohigashi Y, Murai T (2009) Social cognition in schizophrenia: similarities and differences of emotional perception from patients with focal frontal lesions. Eur Arch Psychiatry Clin Neurosci 259:227–233
48. Zahn R, Buechert M, Overmans J, Talazko J, Specht K, Ko CW, Thiel T, Kaufmann R, Dykierek P, Juengling F, Hüll M (2005) Mapping of temporal and parietal cortex in progressive nonfluent aphasia and Alzheimer's disease using chemical shift imaging, voxel-based morphometry and positron emission tomography. Psychiatry Res 140:115–131
49. Zaudig M, Mittelhammer J, Hiller W, Pauls A, Thora C, Morinigo A, Mombour W (1991) SIDAM—a structured interview for the diagnosis of dementia of the Alzheimer type, multi-infarct dementia and dementias of other aetiology according to ICD-10 and DSM-III-R. Psychol Med 21:225–236